Research Article

Eriochrome black adsorption on yellow passion fruit peel (*Passiflora edulis f. Flavicarpa*) treated with sodium hydroxide and nitric acid: study of adsorption isotherms, kinetic models and thermodynamic parameters

Suzana Modesto de Oliveira Brito[1] · José Luiz Cunha Cordeiro[2] · Larissa da Cunha Ramalho[1] · Jéssica Fernanda Ribeiro Oliveira[1]

Abstract
The yellow passion fruit peel was used for Eriochrome black adsorption studies in aqueous solution in such a way as to propose a use for this by-product of the Brazilian fruit juice industry. The passion fruit peel was treated with nitric acid and sodium hydroxide to simulate pectin removal conditions and provide surface modifications that enhance adsorption. The kinetics and equilibrium experiments were completed in batch, at room temperature and contact times from 15 to 240 min. The thermodynamic studies were accomplished through a 298–343 K temperature variation. The adsorption capacities ranged from 196 to 303 mg/g, with the NaOH-treated sample having the highest adsorption capacity at all temperatures. This result points out that the passion fruit peel is a promising adsorbent compared with other low-cost adsorbents. The adsorption process is exothermic and occurs with decreasing entropy. The spontaneity of the process is low except for the sample treated with NaOH. Gibbs free energies were − 1.70 kJ/mol for the untreated sample, − 2.55 kJ/mol for the HNO3-treated sample, and − 6.03 kJ/mol for the NaOH-treated sample at room temperature. The thermodynamic studies have shown that Eriochrome black adsorption on passion fruit peel is a physical process. The process kinetics may be described by the pseudo-second-order model, with diffusion limitations in the solution. The results indicate that NaOH-treated passion fruit peel is a promising adsorbent for Eriochrome black and may be used to adsorb other acid dyes in aqueous medium.

Keywords Passion fruit peel · Acid dye adsorption · Low-cost adsorbents · Fruit peel treatment · Modified passion fruit peel · Isotherm comparison

Mathematical Subject Classification 92E99

JEL Classification Q250 and Q530

✉ Suzana Modesto de Oliveira Brito, smobrito@gmail.com | [1]Universidade Estadual de Feira de Santana, Av. Transnordestina, s/n, Módulo 5, Novo Horizonte, Feira de Santana, Bahia 44036-900, Brazil. [2]Instituto de Química, Universidade Federal da Bahia, Rua Barão de Geremoabo, s/n, Campus Universitário de Ondina, Salvador, Bahia 40170-115, Brazil.

SN Applied Sciences (2019) 1:1226 | https://doi.org/10.1007/s42452-019-1266-x

Received: 13 June 2019 / Accepted: 11 September 2019 / Published online: 17 September 2019

1 Introduction

Several industries use dyes to manufacture their products, especially the textile, tannery, paper and food sectors [1]. Synthetic dyes are widely used due to their advantages over natural dyes [2]. The yearly production of synthetic dyes reaches 700,000 tons/year, and about 10 to 15% of the dyes used by industries reach the effluents [3]. It is expected that the textile industry alone releases approximately 100 tons/year of dyes in aqueous effluents [4]. Depending on concentration and exposure time, dyes may cause allergies, dermatitis and even cancer [5]. Upon release into effluents, they produce an unwanted color in water bodies, reducing photosynthesis processes and harming aquatic life [6].

Effluent treatment containing acid dyes has been widely studied as they represent a growing market and are efficient for coloring cotton. Nevertheless, more than 30% of the dye applied in the dyeing process is lost by hydrolysis in alkaline medium used, and conventional effluent treatment plants are not effective for anionic dye removal [3, 7]. There exists a number of procedures that may be employed to wastewater treatment, as photocatalysis [8–23], electro-coagulation [24, 25] and membrane technology [17, 26].

The adsorption technique has become popular among effluent purification processes owing to their efficiency in removing pollutants resistant to other methods such as dyes. With increasing studies on low-cost adsorbents, this technique has become more feasible [2, 5, 7]. Low-cost adsorbents are considered interesting because they are abundant in nature, available in large quantities and low-priced. Among low-cost adsorbents, biossorbents are those produced from wastes or natural by-products [27]. They were obtained from a variety of materials, since fungi and algae yield by-products or fruit wastes [28].

Lignocellulosic materials appear to behave as good adsorbents, and different physical and/or chemical treatments have been applied to these materials to improve their adsorption capacity [7, 29]. Among these materials, fruit peels produced by processing in the food industry may represent an economical and renewable source of adsorbents for effluents treatment [30]. Various fruit peels have been tested as a low-cost adsorbent, such as orange peel, banana peel and passion fruit peel [3, 29]. Other non-lignocellulosic low-cost adsorbents include bagasse fly ash [31], waste rubber tires [32–34], de-oiled soya [35], Fe_3O_4 nanoparticles [36], guar gum-nano zinc oxide [37], activated carbon [38] among others.

Brazil is the world´s largest passion fruit producer with production outstripping 695,000 tons in 2016 [39–41]. The predominant species is *Passiflora edulis f. flavicarpa*, the popular name of which is yellow passion fruit [42]. Passion fruit juice is the third most consumed beverage in Brazil and keeps the second rank in export [43]. The peel representing 40 to 50% of the fruit weight is considered an industrial waste [43]. This material is rich in essential oils and pectin, and the residue from their extraction may be used as adsorbent.

Pavan et al. [44–46] tested yellow passion fruit peel for methylene blue adsorption and found an adsorption capacity of 44.70 mg g^{-1}. Jacques et al. [47] studied the adsorption of Cr(III) and Pb(II) on passion fruit peel. The maximum adsorption capacity was 85.1 mg g^{-1} and 151.6 mg g^{-1} for Cr(III) and Pb(II), respectively. Gerola et al. [48] studied the adsorption of Pb(II) on passion fruit peel modified with sodium hydroxide and citric acid, verifying an increase in the adsorption capacity for the sample modified with citric acid. The adsorption of acid dyes in fruit peels is scarcely researched in the literature, and there are no reports of this dye adsorption class using passion fruit peel. Eriochrome black T (CI N° 14645, mordant black 11) is used as a dye for wool, silk and nylon fiber and as a complexometric indicator [49].

This article investigates the effect of solution pH parameters, contact time and initial dye concentration in the Eriochrome black adsorption on passion fruit peel treated with nitric acid and sodium hydroxide. The equilibrium data were studied according to the equations of Langmuir, Freundlich, Temkin, Sips and Dubinin–Radushkevich. The process kinetics was studied per the models of pseudo-first order, pseudo-second order, intraparticle diffusion, Elovich and Avrami. The thermodynamic parameters were investigated in order to determine the adsorption process spontaneity.

2 Materials and methods

The Eriochrome black T (molar mass 461.38 g mol^{-1}) was provided by Vetec Química Ltda. Aqueous solutions of concentration ranging from 100 to 1000 mg L^{-1} were

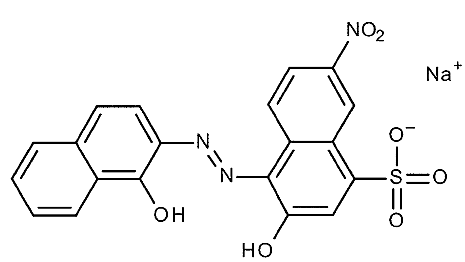

Fig. 1 Structure of the Eriochrome black T. dye. *Source*: Ref. [49]

prepared with deionized water. Figure 1 shows the dye structure.

2.1 Adsorbent treatments

The passion fruit peel samples were ground, washed with deionized water and dried in an oven with air circulation at 150 °C for 24 h to remove more volatile essential oils. A portion of this material was treated with nitric acid 0.1 mol L^{-1} for 90 min at 100 °C under stirring, and another portion was treated with sodium hydroxide 0.1 mol L^{-1} under the same conditions of time and temperature (adapted from Kulkarni et al. [50]). The resulting material was filtered, washed with deionized water and dried at 105 °C for 24 h in ovens with controlled air circulation. The samples were named MF02 (without chemical treatment), MF03 (acid treated) and MF04 (base treated). Each sample underwent grain size separation for further evaluation. The samples were sieved on a vibrating table using 40, 60, 100 and 200 mesh sieves, corresponding to 0.420; 0.250; 0.149 and 0.074 mm particle sizes, respectively.

2.2 pH of zero charge point

The zero charge pH of the samples was determined by the solid addition method as described by Vieira et al. [51]. Twelve vials containing solutions in the pH range of 2 to 13 (pH0) and 0.1 g of adsorbent were stirred for 24 h at room temperature and the final pH was measured with a 10-MB MARTE potentiometer and a glass electrode. The difference between the initial pH and the final pH (DpH) was plotted versus the initial pH and the point where DpH = 0 was taken as pH of zero charge point (pHPZC).

2.3 Effect of mass and granulometry of adsorbent

In order to set the mass to be used in kinetic and thermodynamic studies, a preliminary test was made using Eriochrome black solutions with a concentration of 100 mg L^{-1}, at room temperature, in the four grain sizes obtained for this work. The adsorbent mass varied from 50 to 1500 mg, and the samples were shaken in Erlenmeyers of 100 mL containing 25 mL of the dye solution during 24 h. The sample used for this test was crushed passion fruit peel, washed and dried at 150 °C (MF02), and was used a 6.76 pH, which is equivalent to that of the solution prepared with deionized water.

2.4 Effect of solution pH on adsorption

With the purpose of studying the effect of pH on the adsorption, the pH of the dye solutions was adjusted in the range from 2 to 12 by addition of 0.1 M NaOH or 0.1 M HCl. The solutions, with an initial concentration of 100 mg/L, were then stirred with 0.1 g of adsorbent at room temperature for 24 h. The final concentrations were measured with a spectrophotometer UV/VIS FEMTO 700 Plus and the pH was measured using a 10-MB MARTE potentiometer with a glass electrode. This test used the MF02 sample. No color change of Eriochrome black solution in the pH range used could be observed.

2.5 Kinetic, thermodynamic and adsorption isotherms experiments

In order to evaluate the kinetic models and adsorption isotherms, batch studies were performed using 100-mL Erlenmeyers containing 25 mL of the dye test solution, with initial concentration ranging from 100 to 1000 mg L^{-1}. The adsorbent mass was defined in other experiments as approximately 0.1 g, and the pH of the experiments was always that of the initial solution, ranging from 6.7 to 6.8. The mixture was stirred at room temperature at different contact times. After stirring, the solutions were filtered with paper filter and the final dye concentration was determined using a FEMTO 700 Plus UV/VIS spectrophotometer. Contact times ranged from 15 to 240 min, and experiments with 24 h of agitation were performed, taken as equilibrium time. The adsorption isotherms were built with contact time of 24 h. The effect of temperature on adsorption was investigated in the range of 298–348 K (25–75 °C) as previously described for the batch experiments.

3 Results and discussion

3.1 Effect of mass and granulometry of the adsorbent

Figure 2 shows the effect of adsorbent mass variation on dye removal percentage in the grain sizes obtained for this research. It was observed that percentage of removal increases with decreasing particle size, which was already expected, as smaller particles minimize diffusion limitations and provide greater contact of the adsorbent with the dye, increasing the removal rate. There is an increase in the percentage removal by increasing the adsorbent mass to about 0.1 g. For larger masses, there is barely any increase in dye removal. In accordance with the results of these preliminary tests, the kinetic and thermodynamic experiments used a mass of about 0.1 g of adsorbent in the 0.074 mm particle size for 25 mL of dye solution at concentrations ranging from 100 to 1000 mg/L^{-1}.

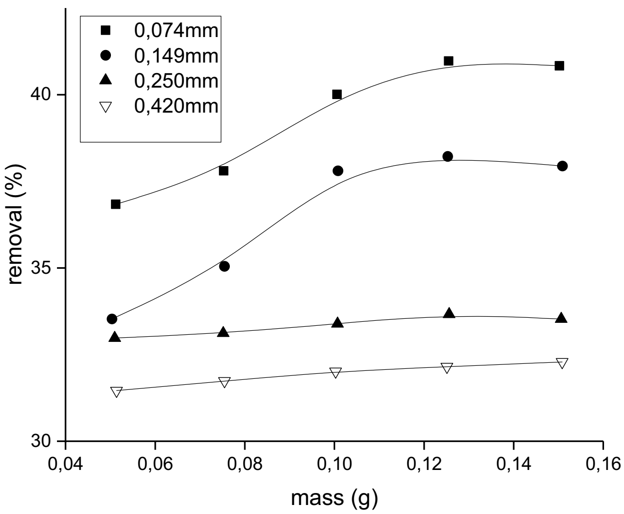

Fig. 2 Removal percentage of Eriochrome black with adsorbent mass for different particle sizes. $Ci = 100$ mg L^{-1}, pH = 6.70; $T = 298$ K, sample MF02

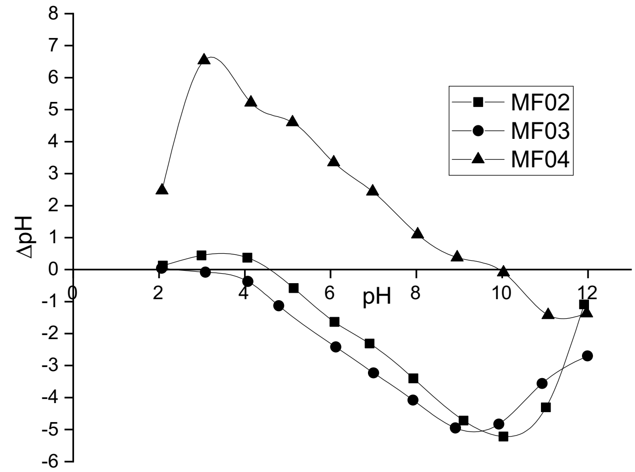

Fig. 3 pH of zero charge point for passion fruit peel samples

Table 1 pH of point of zero charge of yellow passion fruit peel samples

SAMPLE	pH_{PZC}
MF02	4.50 ± 0.01
MF03	2.45 ± 0.01
MF04	9.84 ± 0.01

3.2 Effect of solution pH on adsorption and determination pH of zero charge (PZC) of adsorbent

Adsorption of dye molecules is extremely dependent on pH since the functional groups of the adsorbent surface that are responsible for interaction with these molecules can be protonated or deprotonated to produce different surface charges in solutions with different pH values [52–54]. The pH of the solution may also affect the adsorbate molecule as most dyes go through protonation/deprotonation depending on the medium pH [55].

The pH of the point of zero charge (pH_{PZC}) indicates the adsorbent surface ionization degree and its possible interaction with the adsorbate [55]. Usually, the adsorbent surface becomes positive if it accepts protons from the solution or negative if it loses protons to the solution. The pH where the adsorbent surface is neutral is represented as pH_{PZC} [55]. Figure 3 shows the results of determination of the pH of zero charge point for the passion fruit peel samples used in this study. Table 1 shows the values found for each sample.

The pHPZC of samples MF02 and MF03 is lower than 7, indicating predominantly acidic surfaces. Sample MF04 showed pHPZC higher than 7, indicating that NaOH treatment turned the surface more basic, whereas pHPZC from sample MF03 indicates that the surface became more acidic after HNO_3 treatment. These results suggest that samples MF02 and MF03 would be good adsorbents for basic pollutants, whereas sample MF04 would be a good adsorbent for acid pollutants.

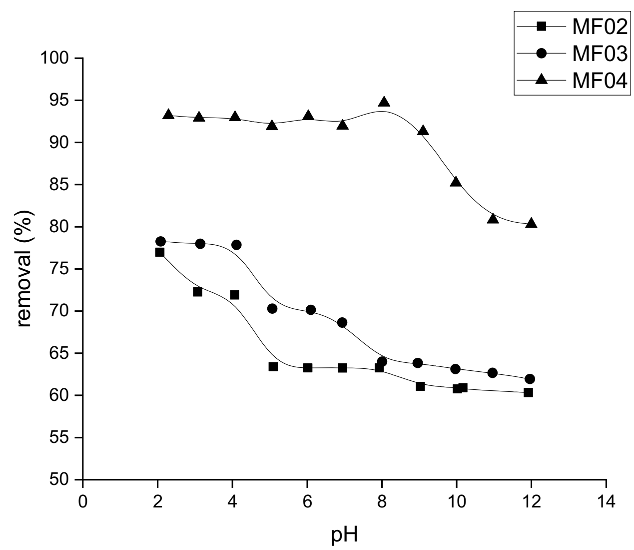

Fig. 4 Effect of pH on Eriochrome black adsorption. $T = 298$ K, $Ci = 100$ mg L^{-1}

Figure 4 shows the effect of pH variation on Eriochrome black sorption on passion fruit samples.

As already expected from the results obtained for pHPZC (Table 1), adsorption is favored for pH ≤ 4.0 except for sample MF04, which presented $pH_{PZC} = 9.84 \pm 0.01$. Srivastava et al. [56] state that cation adsorption is favored at pH > pHPZC because the surface becomes negatively charged, whereas anion adsorption is favored at pH < pHPZC because the surface becomes positively charged. The results obtained in this work confirm this statement and suggest the influence of polarization effects on the adsorption of the colored anion studied. Similar results were found by Munagapati et al. [57] for the adsorption of Congo red over orange peel, Mokhtari et al. [58] for the adsorption of methyl orange on activated carbon impregnated with CuS, Gupta et al. [59] for the adsorption of crystal violet and brilliant green on kaolinite.

Figure 4 shows that the MF02 samples (without treatment) and MF03 (acid treated) exhibit a lower percentage removal across the pH range studied. For these samples, the pH does not influence the adsorption in the pH range 5–7, and a decrease occurs after dye removal with increasing pH. The MF04 sample presented the highest removal rates, with the percentage of removal practically constant in the pH range from 2 to 7, decreasing only from pH = 8.00. Taking into account that between pH = 5.0 and pH = 8.0 the adsorption appears to undergo significant influence of pH, even experiencing a decrease in the percentage removal for MF02 and MF03 samples, kinetic and thermodynamic experiments were accomplished in the original pH of the aqueous solution, which was always close to the pH of the deionized water ranging from 6.5 to 6.8. Such choice simplifies the adsorption system and reduces the cost of adding reagents to adjust the solution pH.

3.3 Study of adsorption isotherms

The Eriochrome black adsorption isotherms on the passion fruit peel samples are shown in Fig. 5, for a contact time of 24 h, pH = 6.8 and room temperature of (298 K). The isotherm model that best fits the adsorption process was studied by adjusting the data obtained from the Langmuir, Freundlich, Dubinin–Radushkevich and Temkin models. The models where the linear regression correlation coefficient (R^2) was closest to the unit were considered adequate to describe the Eriochrome black adsorption system on passion fruit peel.

The Langmuir isotherm and its linearized form may be described by Eqs. 1 and 2, respectively. The Langmuir isotherm presumes monolayer adsorption on sites with equivalent energy [60, 61].

$$Q_e = \frac{Q_{\max} K_L C_e}{1 + K_L C_e} \tag{1}$$

$$\frac{C_e}{Q_e} = \frac{C_e}{Q_{\max}} + \frac{1}{K_l Q_{\max}} \tag{2}$$

The model of Langmuir allows the use of a variable called separation factor (RL), given by Eq. 3:

$$R_L = \frac{1}{1 + K_L C_0} \tag{3}$$

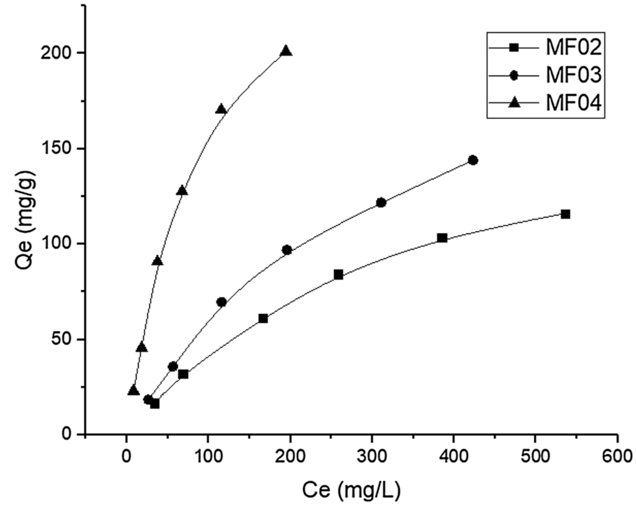

Fig. 5 Adsorption isotherms for Eriochrome black. $T = 298$ K; pH = 6.8; $t = 24$ h

If RL is between zero and 1, that is, 0 < RL < 1, adsorption is said to be favorable. When RL > 1, there is an indication that the solute prefers the liquid phase and adsorption is unfavorable. If RL = 1, we have a linear isotherm, where the amount adsorbed is directly proportional to the equilibrium concentration of adsorbate in the liquid phase [61].

The model of Freundlich considers heterogeneous solid and multilayer adsorption, with adsorption sites of different energies [62, 63]. The isotherm of Freundlich and its linearized equation are represented by Eqs. 4 and 5, respectively.

$$Q_e = K_F C_e^{1/n} \tag{4}$$

$$\ln Q_e = \frac{1}{K_F} + \frac{1}{n} \ln C_e \tag{5}$$

Usually, a favorable adsorption tends to have an n value (Freundlich constant) between 1 and 10. The higher the n value, the stronger the interaction between adsorbate and adsorbent [64].

The Dubinin–Radushkevich isotherm was developed for adsorption of gases and solids and does not consider aspects inherent in the adsorption solution, such as pH and interactions between solute and solvent [64, 65]. The isotherm is given by Eq. 6.

$$Q_e = Q_s \exp\left(-B_{DR}\varepsilon^2\right) \tag{6}$$

And in the linearized form:

$$\ln Q_e = \ln Q_s - B_{DR}\varepsilon^2 \tag{7}$$

where

$$\varepsilon = RT \ln\left(1 + \frac{1}{C_e}\right) \tag{8}$$

The value of the constant k may be associated with average adsorption energy through the equation:

$$E = \frac{1}{\sqrt{2.B_{DR}}} \quad (9)$$

And it may be used to differentiate adsorption as being chemical or physical [66].

The Temkin isotherm takes into account adsorbent–adsorbate interactions and considers that the adsorption heat decreases linearly with increasing surface coverage [67–70]. The expression of the Temkin isotherm is given by Eq. 10 and its linearized form is shown in Eq. 11.

$$Q_e = \frac{RT}{b} \ln \left(a_T C_e \right) \quad (10)$$

$$Q_e = B \ln a_T + B \ln C_e \quad (11)$$

$$B = \frac{RT}{b} \quad (12)$$

The constant B is related to the heat of adsorption and a_T is an equilibrium constant.

Figure 6 shows the linearized isotherms according to the studied models. The parameters achieved for each model are shown in Table 2. From the linear correlation coefficients obtained after the isotherms linearization, we can assume that the Eriochrome black adsorption follows the Langmuir model. The values found for the maximum adsorption capacities (Q_{max}) calculated from the Langmuir isotherm (Table 2) show that treating the samples with acid or with base improves the adsorption capacity of the sample for Eriochrome black.

The RL values achieved at from the Langmuir isotherm are in the range of $0 < RL < 1$ indicating that the Eriochrome black adsorption on passion fruit peel is favorable for all samples. This is confirmed by the n values of the Freundlich equation, which are higher than the unit. The values achieved for the paramenter E of the Dubinin-Radushkevich equation indicate that for all samples the adsorption process is physical. This is confirmed by the factor B values of the Temkin equation.

The adsorbed amount results obtained for samples MF03 and MF04 are significantly higher than for the sample without chemical treatment. The hot treatment of fruit peel in acid medium is one of the methods for pectin extraction found in the literature [71]. As a result, the increased adsorption capacity for the MF03 sample may be attributed to surface modification by pectin extraction, which may have increased the access of molecules to the adsorption sites. The increased adsorption capacity for sample MF04 may be attributed to the surface basicity increase, which favors acid dyes adsorption.

The pH used in the adsorption experiments may also have influenced the Q_{max} results, since the samples MF02 and MF03 have negatively charged surface at pH above 4.50 and 2.45, respectively (Table 1). As the adsorption experiments were performed at pH = 6.8, the surfaces of these materials would be negatively charged, decreasing the adsorption efficiency for anionic dyes. As the sample MF04 has $pH_{PZC} = 9.84$, its surface would be positively charged at the pH used in the adsorption experiments, thus increasing the amount of Eriochrome black adsorbed by this sample. A pH adjustment of the solution, however, would introduce more process costs due to the need for more reagents, thereby failing to meet the requirements of low-cost adsorption processes.

Table 3 shows a comparison of the maximum adsorption capacity of Langmuir to Eriochrome black over various adsorbents. Adsorption capacities are shown in increasing order. As can be seen, although there are adsorbents with higher adsorption capacity than passion fruit peel, the NaOH-treated material has one of the highest adsorption capacities of the materials presented here. Comparison was made for adsorption of Eriochrome black in similar conditions. Although our materials are not the best adsorbent, it has better adsorption capacity than numerous materials, including graphene and lamellar double hydroxides. Among lignocellulosic materials found to adsorb Eriochrome black, our material is the best one.

3.3.1 Kinetic studies

The Eriochrome black adsorption was studied as a function of contact time to determine the kinetic model that best describes the adsorption process. The results of variation in amount adsorbed over time and with initial concentrations are shown in Fig. 7. The results in Fig. 7 show that Eriochrome black adsorption reaches equilibrium in about 60 min for all samples passion fruit peel. The adsorbed amount increases with increasing initial concentration for all samples.

The kinetics of this process of adsorption was studied by the models of pseudo-first order, pseudo-second order, Elovich, Boyd and intraparticle diffusion. The adsorption kinetic modeling is shown here for the initial concentration of Eriochrome black 100 mg/L^{-1}.

Equation 13 shows the pseudo-first-order model proposed by Lagergren in its linear form [80].

$$\log \left(Q_e - Q_t \right) = \log Q_e - \frac{k_{ad}}{2,303} t \quad (13)$$

where Q_e and Q_t are the adsorbed amounts at equilibrium and time t (mg/g); kad is the adsorption velocity constant (min^{-1}); and t is the time (min).

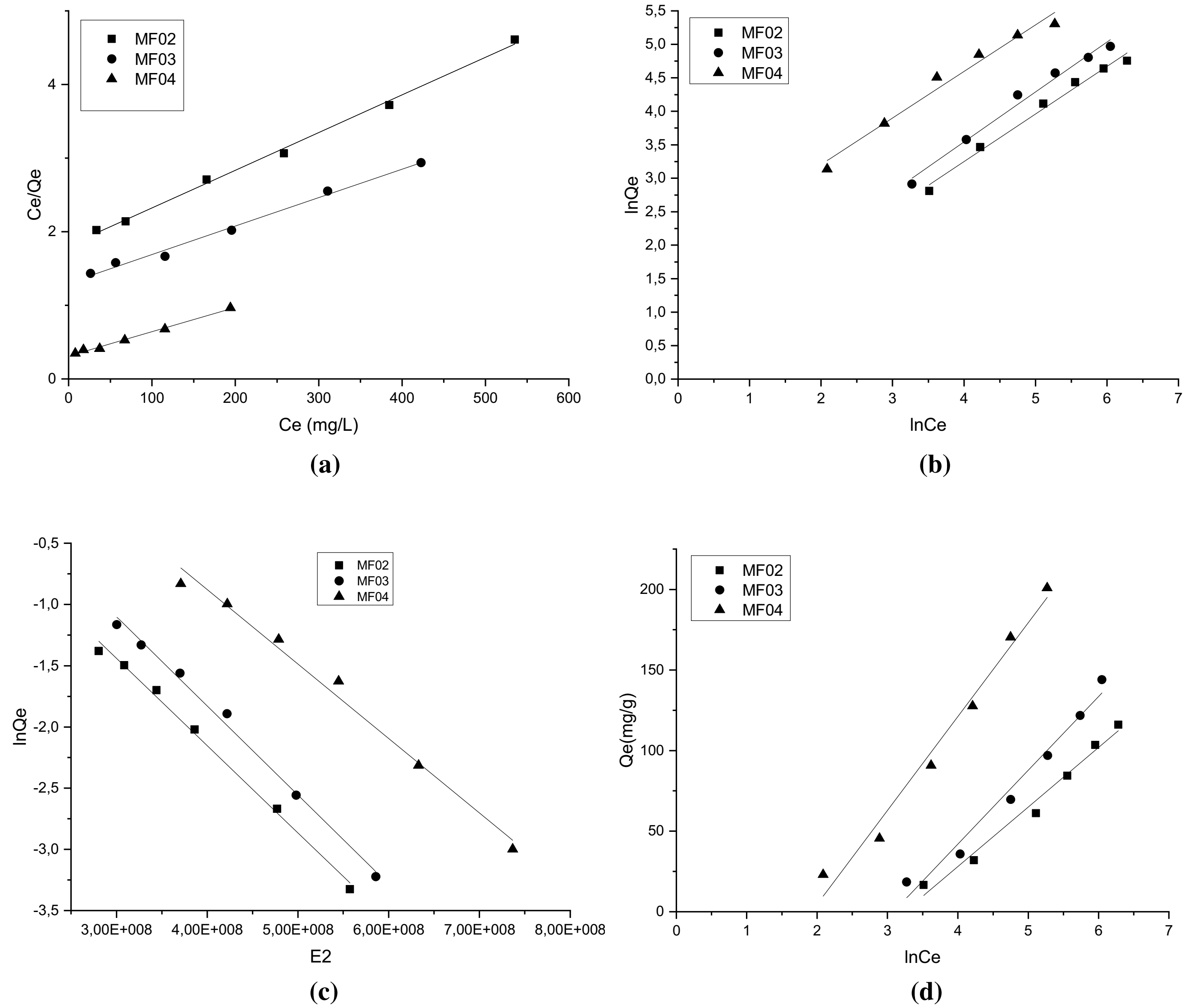

Fig. 6 Linearization of isotherms according to Langmuir (**a**), Freundlich (**b**), Dubinin–Radushkevich (**c**) and Temkin (**d**). $T=298$ K, pH = 6.8, $t=24$ h

Ho et al. [80–83] proposed that the pseudo-second-order model better describes the adsorption of dyes on low-cost materials. Equation 14 shows one form of the linear model proposed by Ho [83].

$$\frac{t}{Q_t} = \frac{1}{k_2.Q_e^2} + \frac{1}{Q_e}.t \tag{14}$$

where Q_e and Q_t are the adsorbed amounts (mg g^{-1}) at equilibrium and at time t (min) and k is the pseudo-second-order rate constant (g mg^{-1} min^{-1}).The linear form of the Elovich equation is given by:

$$Q = \frac{1}{\beta}\ln(\alpha.\beta) + \frac{1}{\beta}\ln t \tag{15}$$

where Q is the amount adsorbed per gram of adsorbent (mg/g), α is the initial rate of adsorption (mg/g.min), β is a constant related to desorption of the surface coverage and the activation energy adsorption (g/mg) [84]. The Elovich equation neglects desorption and seems to better describe adsorption on heterogeneous surfaces [85].

The following figures show the graphs obtained for the kinetic modeling of the adsorption process studied in this research. Table 4 shows the parameters obtained for this modeling. Due to room unavailability, graphs and data are shown only for the initial concentration of 100 mg L^{-1}.

Figure 8 shows the graph obtained for pseudo-first-order modeling at room temperature and initial concentration of Eriochrome black 100 mg/L.

Table 2 Parameters obtained from adsorption isotherms for Eriochrome black on passion fruit samples

Isotherm	Parameters	MF02	MF03	MF04
Langmuir	Q_{max} (mg/g)	196.08 ± 0.01	256.41 ± 0.003	303.03 ± 0.02
	K_L (L/mg) × 10^3	2.81 ± 0.03	2.99 ± 0.01	10.50 ± 0009
	R_L	0.26	0.25	0.09
	R^2	0.9966	0.9915	0.9939
Freundlich	n	1.4	1.3	1.4
	K_F (mg/g) (L/mg)$^{1/n}$	2.46 ± 0.02	1.78 ± 0.01	0.55 ± 0.006
	R^2	0.9869	0.9858	0.9742
Dubinin–Radushkevich	B_{DR} × 10^9 (mol^2/kJ^2)	7.12 ± 0.02	7.27 ± 0.03	6.07 ± 0.02
	Q_s (mmol/g)	2.01 ± 0.02	2.95 ± 0.01	4.73 ± 0.01
	E (kJ/mol)	8.37 ± 0.02	8.29 ± 0.01	9.07 ± 0.008
	R^2	0.9951	0.9942	0.9869
Temkin	B (J/mol)	36.94 ± 0.03	45.82 ± 0.03	58.26 ± 0.02
	a_T (L/mg)	0.0391	0.0458	0.0465
	R^2	0.9808	0.9765	0.9809

T = 298 K, pH = 6.8; t = 24 h

Table 3 Maximum adsorption capacities (Langmuir) of Eriochrome black on various adsorbents

Adsorbent	Q_{max} (mg/g)	Ref.
Nteje Clay	16.26	[72]
Sawdust	40.96	[73]
Acid-modified graphene	58.64	[74]
$NiFe_2O_4$NPs	81.52	[75]
Graphene	85.55	[74]
NiFe-CLDH	132.49	[76]
H_3PO_4-modified berry leaves	133.33	[77]
Sludge-derived activated carbon	178.2	[78]
MF02	196.08	This work
MF03	256.41	This work
MF04	303.03	This work
CoAl-CLDH	419.87	[76]
Date palm ash MgAL-LDH	425.16	[79]
MgAl-CLDH	540.91	[76]

The linear plots of $\log_{10}(Q_e - Q_t)$ versus t showed very low linear correlation coefficients, indicating that this model does not describe the Eriochrome black adsorption kinetics on different samples passion fruit peel. Even in the samples in which the correlation coefficient approached unity (between 0.95 and 0.97), the calculation of the adsorbed amount at equilibrium (Q_e) showed results very far from those obtained experimentally, confirming that the pseudo-first-order model is not proper to describe the results achieved.

Figure 9 shows the graph obtained for pseudo-second-order modeling for Eriochrome black adsorption on passion fruit peel samples at room temperature and initial dye concentration of 100 mg L^{-1}.

The results obtained for the correlation coefficients were higher than 0.999 for all samples tested, indicating that the pseudo-second-order model describes well the Eriochrome black adsorption on passion fruit peel. The pseudo-second-order model is considered more experimental than theoretical, being applicable to systems where the experimental simulation is close to real conditions. The pseudo-second-order model also assumes that there may be ion exchange between adsorbate and adsorbent. However, the thermodynamic data shown in the next section does not indicate which chemical processes are occurring in this system. Accordingly, the pseudo-second-order model is a good mathematical description of the process, but obscures the adsorption mechanism taking place. This assumption is supported by several works in the literature, as the adsorption of Eriochrome black [79, 86].

Figure 10 shows the graph obtained for the study of Eriochrome black adsorption data on passion fruit peel according to the linearized Elovich equation.

The R^2 values for Elovich modeling were very low compared to the pseudo-second-order model, indicating that this equation is not proper to describe the Eriochrome black adsorption kinetics on passion fruit peel. The α values were extremely high, which would correspond to a very fast initial adsorption that is confirmed by the low values of t_0.

The results obtained for the other initial concentrations showed that the expected increase in the constants α and β with the increase in the initial concentration [84] did not occur, and the obtained values varied randomly. Yet, the values of the Elovich constants found in this paper do not agree with values obtained in similar conditions [87, 88]. Based on these results, it is considered that the Elovich

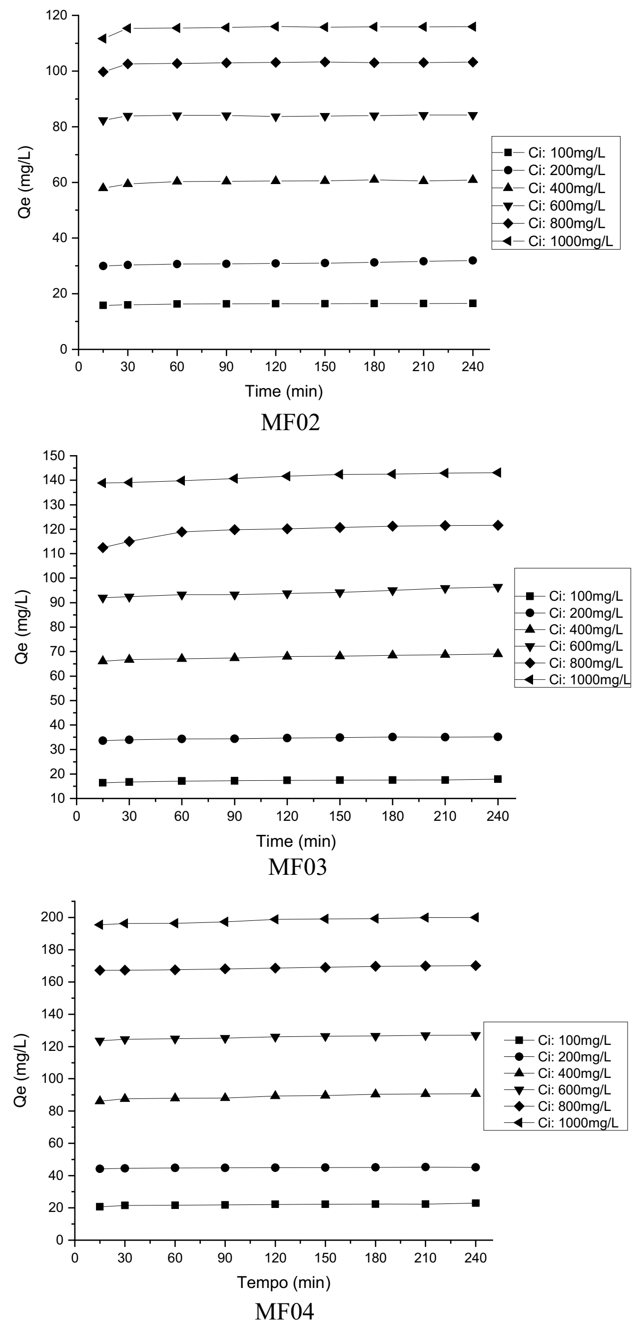

Fig. 7 Changes in the amount of Eriochrome black adsorbed with the contact time and with the initial concentrations for the passion fruit peel samples. $T=298$ K, pH = 6.8, $Ci=100$ to 1000 mg L^{-1}

model does not describe the adsorption process kinetics studied in this work.

The adsorption mechanism is not always clear from the models used in this study. Furthermore, liquid-phase adsorption is always subject to rate-limiting steps such as film diffusion and intraparticle diffusion. In order to study the rate-limiting step of this process, models of Boyd and Weber and Morris were used.

Boyd diffusion model [89] determines how much resistance to mass transfer is in the film surrounding the adsorbent particle or the diffusion inside the pores. This model can be expressed by equation:

$$f = 1 - \frac{6}{\pi^2}\sum_{n=1}^{\infty}\frac{1}{n^2}\exp\left(-n^2Bt\right) \tag{16}$$

$$f = \frac{Q_t}{Q_e} \tag{17}$$

where f is the equilibrium fraction reached at different times (t) and Bt is a function of f. Q_e and Q_t are the quantities adsorbed at time t and at equilibrium, respectively (mg/g).

Reichenberg (1953) [90] obtained the following approximations to allow the calculation of Bt:

$$\text{For } f > 0.85 \quad Bt = -0.4977 - \ln(1-f) \tag{18}$$

$$\text{For } f < 0.85 \quad Bt = \left(\sqrt{\pi} - \sqrt{\pi - \frac{\pi^2 f}{3}}\right)^2 \tag{19}$$

A plot of Bt versus time can be used to obtain information about the adsorption process mechanism. If the graph is linear and passes through the origin, the pore diffusion controls the mass transfer rate. If the graph is nonlinear or linear, but does not pass through the origin, film diffusion or chemical reactions control the adsorption rate [91].

Figure 11 shows the graph obtained for applying the Boyd equation [89] to the experimental data for initial concentration of 100 mg L^{-1}. Table 5 summarizes the values found for B and for the diffusion coefficient. (D_i), calculated by the expression:

$$B = \frac{\pi^2 D_i}{r^2} \tag{20}$$

where r is the radius of the molecule (m) assuming it has a spherical shape.

The plot of Bt versus t for Eriochrome black adsorption on passion fruit peel showed low linearity and does not go through the origin. This behavior indicates that the adsorption is controlled by external mass transfer and not by particle pore diffusion, which was already expected, since the passion fruit peel particles do not have a defined pore structure. This consideration is reinforced by the low values of B found, which resulted in values for the diffusion coefficient, D_i, also very low, indicating that the diffusion of the molecule in the solution is slow.

Diffusion processes can also be investigated using the Weber–Morris model [92], described by Eq. 21:

Table 4 Parameters obtained for the kinetic modeling of Eriochrome black adsorption on passion fruit bark

Kinetic model	Parameters	MF02	MF03	MF04
Pseudo-first order	k_{ad} (min^{-1}) × 10^3	9.21 ± 0.01	5.07 ± 0.05	9.44 ± 0.02
	Q_e (mg/g)	0.78	1.95	2.56
	Q_e EXP (mg/g)	16.61 ± 0.02	18.40 ± 0.01	23.02 ± 0.01
	R^2	0.9314	0.9070	0.7371
Pseudo-second order	k_2 (g/mg min) × 10^2	6.00	2.10	1.56
	Q_e (mg/g)	16.58	17.89	22.83
	Q_eEXP (mg/g)	16.61 ± 0.02	18.40 ± 0.01	23.02 ± 0.01
	R^2	1.0000	0.9997	0.9995
Elovich	t_0 (min)	5.2×10^{-27}	1.14×10^{-13}	1.77×10^{-13}
	B (g/mg)	4.15	2.07	1.58
	A (mg/g min)	7.26×10^{26}	1.81×10^{13}	8.95×10^{12}
	R^2	0.9517	0.9635	0.9306

Ci = 100 mg L^{-1}, *T* = 298 K, pH = 6.8

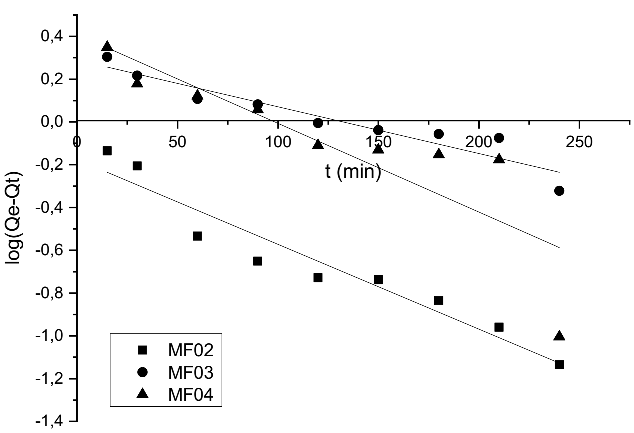

Fig. 8 Plot of pseudo-first order for Eriochrome black adsorption on passion fruit peel. *Ci* = 100 mg/L, *T* = 298 K, pH = 6.8

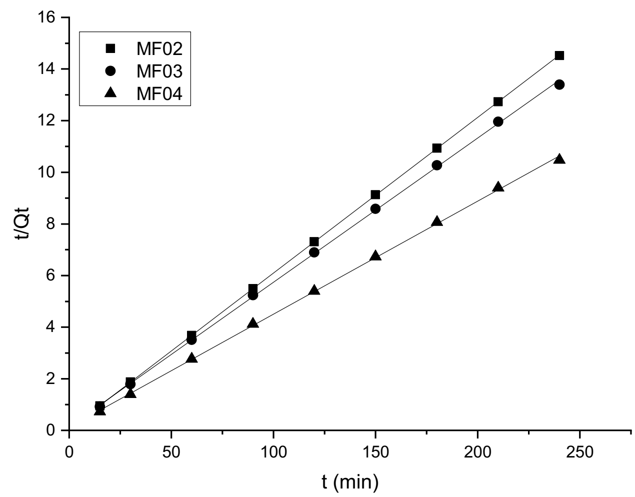

Fig. 10 Elovich plot for adsorption of Eriochrome black on passion fruit samples. *Ci* = 100 mg/L; *T* = 298 K, pH = 6.8

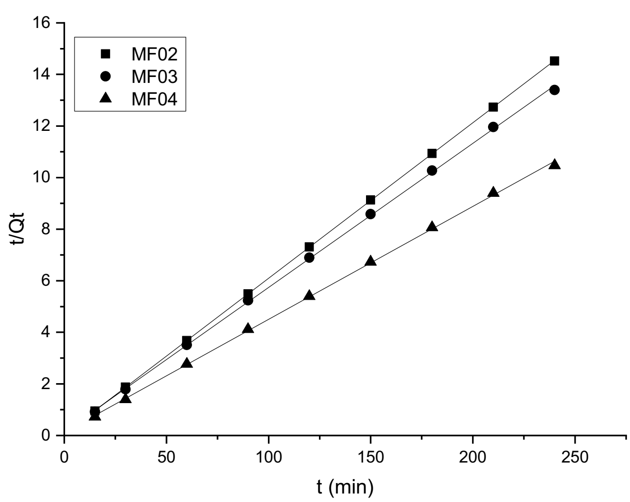

Fig. 9 Pseudo-second-order plot for adsorption of Eriochrome black on passion fruit bark. *Ci* = 100 mg/L, *T* = 298 K, pH = 6.8

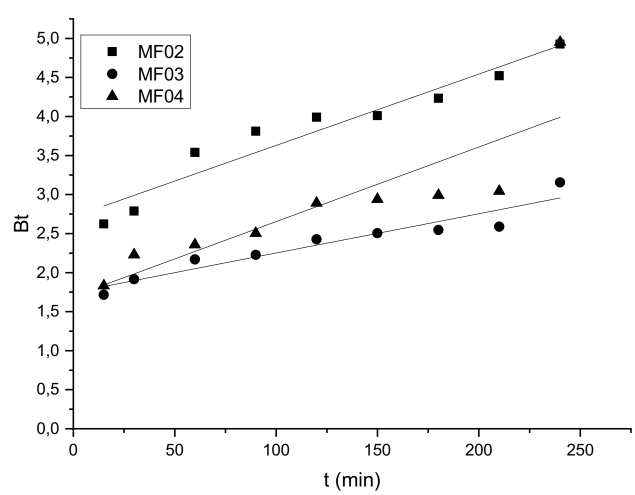

Fig. 11 Boyd plots for adsorption of Eriochrome black on passion fruit bark, *Ci* = 100 mg L^{-1}, *T* = 298 °C, pH = 6.8

Table 5 Parameters obtained for mathematical modeling by equations of Boyd and Weber–Morris

Model	Parameters	MF02	MF03	MF04
Boyd	B	0.0091	0.0050	0.0096
	D_i (m²/min)	1.31×10^{-12}	7.24×10^{-13}	1.37×10^{-12}
	R^2	0.9314	0.9069	0.7371
Weber and Morris	$k_{i\,1}$ (mg g^{-1} min$^{-1/2}$)	01155	0.1871	0.1865
	C_1 (mg/g)	15.399	15.686	20.2108
	R_1^2	0.9671	0.9903	0.9912
	$k_{i.2}$ (mg g^{-1} min$^{-1/2}$)	0.0259	0.0702	0.0374
	C_2 (mg/g)	16.122	16.581	21.821
	R_2^2	0.9704	0.9560	0.9661

$$Q_t = k_i\sqrt{t} + c \tag{21}$$

where k_i is the intraparticle diffusion velocity constant (mol g^{-1} min$^{-1/2}$). A graph of Q_t versus $t^{1/2}$ must be a straight line, the slope of which gives the value of the diffusion constant. If $c \neq 0$ intraparticle diffusion is not the only process controlling the velocity [80].

Figure 12 shows Weber–Morris plots for the Eriochrome black adsorption process on the samples tested at an initial concentration of 100 mg/L, pH = 6.8 and room temperature (298 K).

It can be observed that the graphs are linear, but do not go through the origin, indicating that intraparticle diffusion is not the main factor determining the adsorption velocity. The graphs show two diffusion steps, which can be attributed to solution diffusion and diffusion in the liquid film surrounding the particle. The result set shows that the limiting step in the process was probably diffusion in the solution.

As a result, the kinetic studies indicate that the process kinetics can be mathematically described by the pseudo-second-order model, but that the diffusional limitations in the solution, which may be due to the agitation speed used in the experiments, are influencing the process.

3.4 Thermodynamic studies

Figures 13, 14 and 15 show the Eriochrome black adsorption isotherms, respectively, for samples MF02 to MF04, at the temperatures studied in this work.

The amount adsorbed decreases with increasing temperature as expected for an exothermic process. Thermodynamic parameter values, enthalpy, entropy and Gibbs free energy, as well as the equilibrium constants, were determined using Eqs. 22 to 24 [53, 93] and are summarized in Table 6.

$$\log K_C = -\frac{\Delta H^0}{2.303RT} + \frac{\Delta S^0}{2.303R} \tag{22}$$

$$\Delta G^0 = -RT \ln K_C \tag{23}$$

$$K_C = \frac{C_{ads}}{C_e} \tag{24}$$

Thermodynamic studies' results indicate that the adsorption process is exothermic for all samples tested, supporting the results of decreased adsorption capacity with increasing temperature shown in Figs. 13, 14 and 15. The process occurs with decreased entropy, which was expected as the molecules are more organized when adsorbed on the surface than in solution.

The results obtained for Gibbs free energy indicate that the Eriochrome black adsorption on the various samples is spontaneous at low temperatures, becoming less and less spontaneous as the temperature increases. This result confirms the assumption that the process is primarily physical adsorption. Other works reported the same behavior, considering that interaction of Eriochrome black with adsorbents is from electrostatically nature [73].

4 Conclusions

Passion fruit peel proved to be a promising adsorbent for Eriochrome black dye, with adsorption capacities ranging from 196 to 303 mg dye per gram of adsorbent. Generally, the treatment of the sample with acid or base improves the adsorption capacity, but the base treatment was more effective in increasing the adsorption capacity. The process

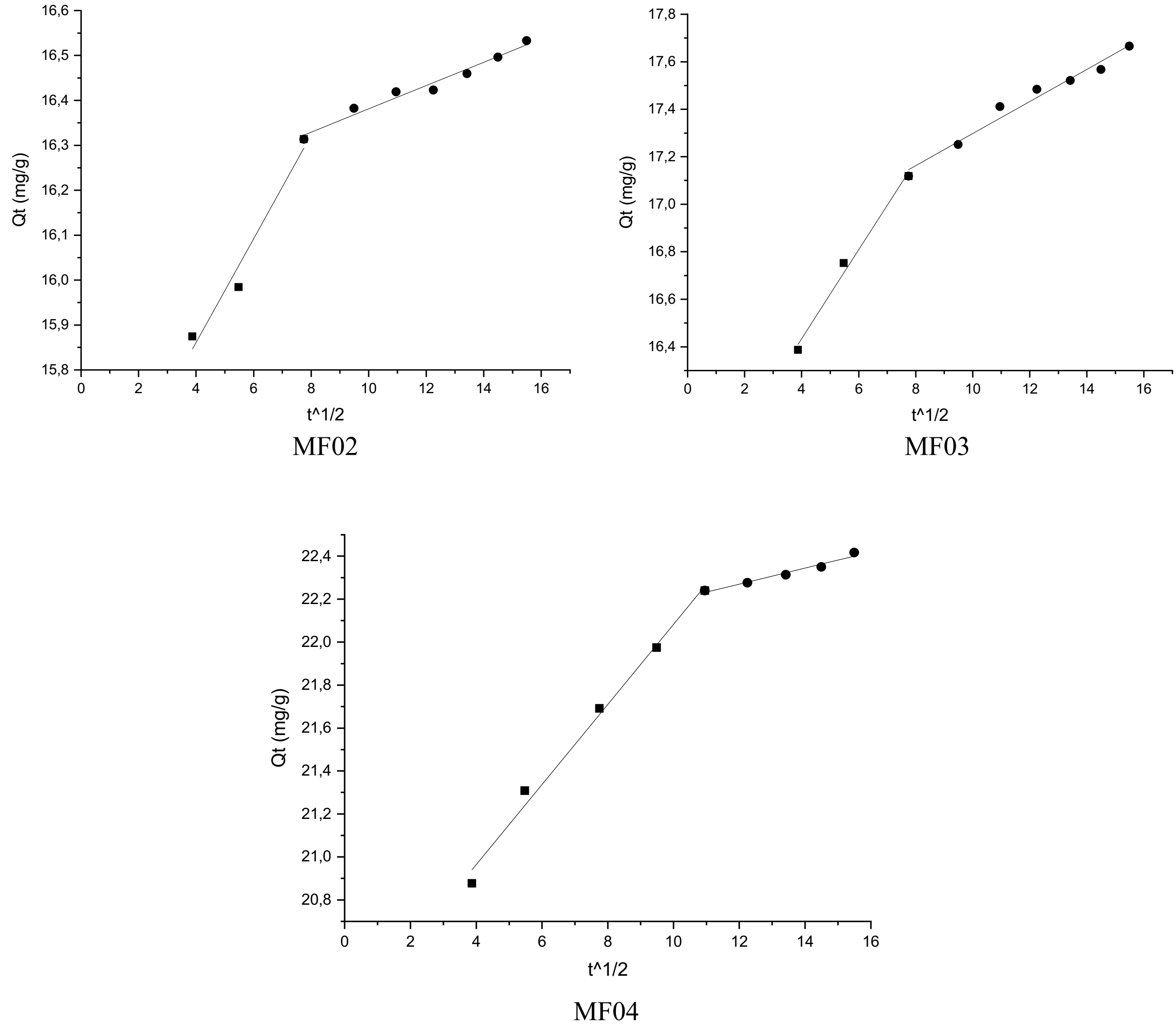

Fig. 12 Weber–Morris diagrams for adsorption of Eriochrome black on passion fruit bark. $Ci = 100$ mg/L, $T = 298$ K, pH = 6.8

kinetics may be described mathematically by the pseudo-second-order equation, and diffusion studies have shown that diffusion in the solution is influencing the results, being the process velocity a limiting step. Eriochrome black adsorption on passion fruit peel is an exothermic process, which occurs with decreased entropy, and the obtained Gibbs free energies indicate that the process is spontaneous at temperatures close to room temperatures (298 K).

Comparison with other Eriochrome black adsorption processes reported in the literature shows that passion fruit peel can be employed as adsorbent for this dye and that the base treatment produces the best material for the adsorption process at room temperature. The results of this study show that the passion fruit peel may be a good adsorbent for other acid dyes beyond the Eriochrome black.

Acknowledgements Dr. Suzana Modesto de Oliveira Brito, professor at State University of Feira de Santana, wishes to thank State University of Feira de Santana for providing the support needed for our experimental studies.

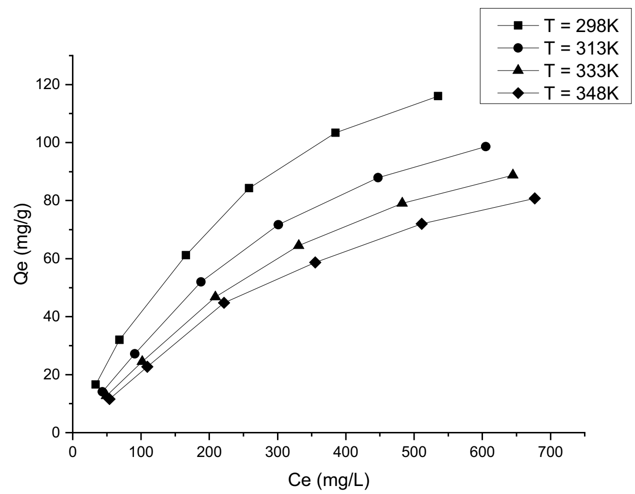

Fig. 13 Adsorption isotherms for the sample MF02 at the temperatures used in this work

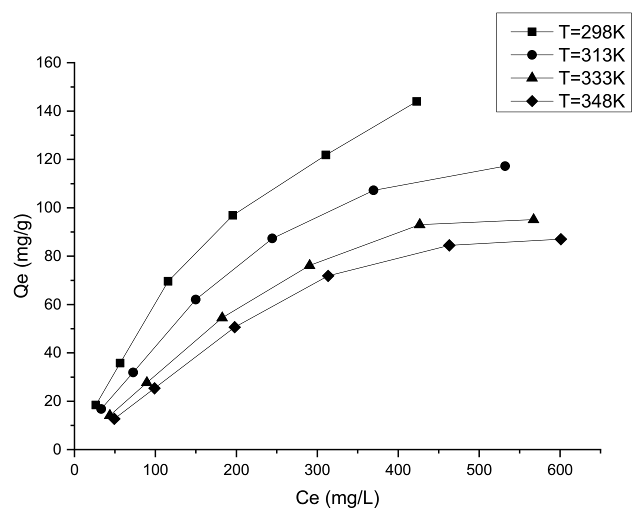

Fig. 14 Adsorption isotherms for the sample MF03 at the temperatures used in this work

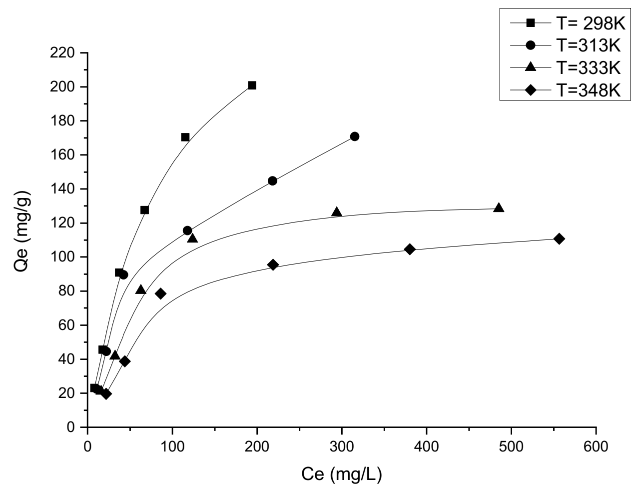

Fig. 15 Adsorption isotherms for the sample MF04 at the temperatures used in this work

Table 6 Thermodynamic parameters obtained for adsorption of Eriochrome black on passion fruit peels

Sample	*T* (°C)	K_C	Δ*H*° (kJ/mol)	Δ*S*° (J/K mol)	Δ*G*° (kJ/mol)
MF02	298	0.87	−9.94	−34.78	0.34
	313	0.65			1.10
	333	0.55			1.64
	348	0.48			2.73
MF03	298	1.37	−11.67	−37.28	−0.77
	313	0.88			0.33
	333	0.76			0.74
	348	0.66			1.18
MF04	298	4.15	−28.89	−85.53	−3.53
	313	2.17			−2.02
	333	1.06			−0.17
	348	0.80			0.65

Compliance with ethical standard

Conflict of interest The authors declare that they have no conflict of interest.

Human and animal rights This research did not involve humans or animals.

References

1. Ahmaruzzaman M, Gupta VK (2011) Rice Husk and its ash as low-cost adsorbents in water and wastewater treatment. Ind Eng Chem Res 50:13589–13613
2. Kyzas GZ, Fu J, Matis KA (2013) The change from past to future for adsorbent materials in the treatment of dyeing wastewaters. Materials 6:5131–5158
3. Kharat DS (2015) Preparing agricultural residue-based adsorbents for dyes from effluents—A review. Braz J Chem Eng 1:1–12
4. Yagub MT, Sen TK, Ang HM (2012) Equilibrium, kinetics, and thermodynamics of methylene blue adsorption by pine tree leaves. Water Air Soil Pollut 223:5267–5282
5. Bharathi KS, Ramesh ST (2013) Removal of dyes using agricultural waste as low-cost adsorbents: a review. Appl Water Sci 3:773–790
6. Yagub MT, Sen TK, Afroze S, Ang HM (2014) Dye and its removal from aqueous solution by adsorption: a review. Adv Colloid Interface Sci 209:172–184
7. Gupta V (2009) Application of low-cost adsorbents for dye removal—a review. J Environ Manag 90(8):2313–2342

8. Saravanan S, Sacari E, Gracia F, Khan MM, Mosquera E, Gupta VK (2016) Conducting PANI Stimulated ZnO System for visible light photocatalytic degradation of coloured dyes. J Mol Liq 221:1029–1033
9. Saravanan R, Khan MM, Gracia F, Qin J, Gupta VK, Arumainathan S (2016) Ce^{3+}-ion-induced visible-light photocatalytic degradation and electrochemical activity of ZnO/CeO_2 nanocomposite. Sci Rep 6:31641
10. Saravanan R, Khan MM, Gupta VK, Mosquera E, Gracia F, Narayanan V, Stephen A (2015) J Colloid Interface Sci 452:126–133
11. Saravanan R, Khan MM, Gupta VK, Mosquera E, Gracia F, Narayanan V, Stephen A (2015) ZnO/Ag/Mn_2O_3 nanocomposite for visible-light induced industrial textile effluent degradation, uric acid and ascorbic acid sensing and antimicrobial activity. RSC Adv 44:34645–34651
12. Saravanan R, Gupta VK, Narayanan V, Stephen A (2014) Visible light degradation of textile effluent using novel catalyst ZnO/γ-Mn_2O_3. J Taiwan Inst Chem Eng 45(4):1910–1917
13. Saravanan R, Karthikeyan VK, Gupta VK, Sekaran G, Narayanan V, Stephen A (2013) Enhanced photocatalytic activity of ZnO/CuO nanocomposite for the degradation of textile dye on visible light illumination. Mater Sci Eng C 33:91–98
14. Saravanan R, Karthikeyan VK, Gupta VK, Thirumal E, Thangadurai P, Narayanan V, Stephen A (2013) ZnO/Ag nanocomposite: an efficient catalyst for degradation studies of textile effluents under visible light. Mater Sci Eng C 33:2235–2244
15. Saravanan R, Gupta VK, Prakash T, Narayanan V, Stephen A (2013) Synthesis, characterization and photocatalytic activity of novel Hg doped ZnO nanorods prepared by thermal decomposition method. J Mol Liq 178:88–93
16. Saravanan R, Thirumal E, Gupta VK, Narayanan V, Stephen A (2013) The phtocatalytic activity of ZnO prepared by simple thermal decomposition method at various temperatures. J Mol Liq 177:394–401
17. Saleh TA, Gupta VK (2012) Photo-catalyzed degradation of hazardous dye methyl orange by use of a composite catalyst consisting of multi-walled carbon nanotubes and titanium dioxide. J Colloid Interface Sci 371:101–106
18. Saleh TA, Gupta VK (2011) Functionalization of tungsten oxide into MWCNT and its application for sunlight-induced degradation of rhodamine-B. J Colloid Interface Sci 362:337–344
19. Gupta VK, Jain R, Nayak A, Agarwal S, Shrivastava M (2011) Removal of the hazardous dye—Tartrazine by photodegradation on titanium dioxide surface. Mater Sci Eng C 31:1062–1067
20. Gupta VK, Atar M, Yola ML, Ustundag Z, Uzun L (2014) A novel magnetic Fe@Au core-shell nanoparticles anchored graphene oxide reciclable nanocatalyst for the reduction of nitrophenol compounds. Water Res 48:210–217
21. Saravanan R, Joicy S, Gupta VK, Narayanan V, Stephen A (2013) Visible light induced degradation of methylene blue using CeO_2/V_2O_5 and CeO_2/CuO catalysts. Mater Sci Eng C 33:4725–4731
22. Saravanan R, Gupta VK, Narayanan V, Stephen A (2013) Comparative study on photocatalytic activity of ZnO prepared by different methods. J Mol Liq 181:133–141
23. Saravanan R, Gupta VK, Mosquera E, Gracia F (2014) Preparation and characterization of V_2O_5/ZnO nanocomposite system to photocatalytic application. J Mol Liq 198:409–412
24. Ali I, Asim M, Khan TA (2013) Arsenite removal from water by electro-coagulation on zin-zin and copper-copper electrodes. Int J Environ Sci Technol 10:377–384
25. Devaraj M, Saravanan R, Deivasigamani R, Gupta VK, Gracia F, Jayadevan S (2016) Fabrication of novel shape Cu and Cu/Cu_2O nanoparticles modified electrode for the determination of dopamine and paracetamol. J Mol Liq 221:930–941
26. Saleh TA, Gupta VK (2012) Synthesis and characterization of alumina nano-particles polyamide membrane with enhanced flux reflection performance. Sep Pur Tech 89:245–251
27. Crini G, Lichtfouse E, Wilson LD, Morin-Crini N (2019) Conventional and non-conventional adsorbents for wastewater treatment. Environ Chem Lett 17(1):195–201
28. Gupta VK, Nayak A, Agarwal S (2015) Bioadsorbents for remediation of heavy metals: current status and their future prospects. Environ Eng Res 20(1):001–018
29. Saba B, Christy AD, Jabeen M (2016) Kinetic and enzimatic decolorization of industrial dyes utilizing plant-based biosorbents: a review. Environ Eng Sci 33:601–614
30. Bhatnagar A, Silanpaa M, Witek-Krowiak A (2015) Agricultural waste peels as versatile biomass for water purification—A review. Chem Eng J 270:244–271
31. Gupta VK, Jain CK, Ali I, Chandra S, Agarwal S (2002) Removal of lindane and malathion from wastewater using bagasse fly ash—a sugar industry waste. Water Res 36:2483–2490
32. Gupta VK, Ali I, Saleh TA, Siddiqui MN, Agarwal S (2013) Chro-9mium removal from water by activated carbon developed from waste rubber tires. Environ Sci Pollut Res 201:1261–1268
33. Gupta VK, Nayak A, Agarwal S, Tyagi I (2014) Potential of activated carbono from waste rubber tire for the adsorption of phenolics: effect of pre-treatment conditions. J Colloid Interface Sci 417:420–430
34. Saleh TA, Gupta VK (2014) Processing methods, characteristics and adsorption behavior of tire derived carbons: a review. Adv Colloid Interface Sci 211:93–101
35. Mittal A, Mittal J, Maloiya A, Gupta VK (2010) Removal and recovery of chrysoidine Y from aqueous solutions by waste materials. J Collid Interface Sci 344:497–507
36. Ghaedi M, Hajjtati S, Mahmudi Z, Tyagi I, Agarwal S, Maity A, Gupta VK (2015) Modelling of competitive ultrasonic assisted removal of the dyes methylene blue and safranin-o using Fe_3O_4 nanoparticles. Chem Eng J 268:28–37
37. Khan TA, Nazir M, Ali I, Kumar A (2017) Removal of chromium VI from aqueous solution using guar gum-nanozinc oxide biocomposite adsorbent. Arabi J Chem 10:52388–52398
38. Asfaram A, Ghaedi M, Agarwal S, Tyagi I, Gupta VK (2015) Removal of basic dye auramine-o by ZnS: cu nanoparticles loaded activated carbon. Optimization of parameters using response surface methodology with central composite design. RSC Adv 5:18438–18450
39. Fraife Filho GA, Leite JBV, Ramos JV (2015) Passion fruit. 2015. CEPLAC: http://www.ceplac.gov.br/radar/maracuja.htm. Accessed on August 31, 2015
40. EMBRAPA. (2015). Passion fruit. Portal EMBRAPA: https://www.embrapa.br/mandioca-e-fruticultura/cultivos/maracuja. Access on August 31, 2015
41. Carvalho C, Kist BB, Santos CE, Treichel M, Filter CF (2017) Brazilian yearbook of fruticulture. Gazeta, Santa Cruz do Sul
42. Meletti LM (2011) Advances in the Culture of Passion Fruit in Brazil. Revista Brasileira de Fruticultura, Special Volume E, 83-91
43. SEBRAE Portal: http://www.sebrae.com.br/sites/PortalSebrae/artigos/culture-the-market-of-maracuja,108da5d3902e2410VgnVCM100000b272010aRCRD.. Accessed on October 11, 2017
44. Pavan FA, Gushikem Y, Mazzocato AC (2007) Statistical design of experiments as a tool for optimizing the batch conditions to methylene blue biosorption on yellow passion fruit and mandarin peels. Dyes Pigm 72:256–266
45. Pavan FA, Mazzocato AC, Gushikem Y (2008) Removal of methylene blue dye from aqueous solutions by adsorption using yellow passion fruit peel as adsorbent. Biores Technol 99:3162–3165

46. Pavan FA, Lima EC, Dias SL, Mazzocato AC (2008) Methylene blue biosorption from aqueous solutions by yellow passion fruit waste. J Hazard Mat 150:703–712
47. Jacques RA, Lima EC, Dias SLP, Mazzocato AC, Pavan FA (2007) Yellow passion fruit shell as biosorbent to remove Cr(III) and Pb(II) from aqueous solution. Sep Pur Tech 57:193–198
48. Gerola GP, Vilas Boas N, Caetano J, Tarley CRT, Gonçalves C Jr, Dragunski DC (2013) Utilization of passion fruit skin by-product as lead (II) ion biosorbent. Water Air Soil Pollut 224:1446–1456
49. World dye variety. Mordant Black 11, http://www.worlddyevariety.com/mordant-dyes/mordant-black-11.html. Accessed on 31 August 2016
50. Kulkarni SG, Vijayanand P (2010) Effect of extraction conditions oh the quality characteristics of pectin from passion fruit peel (*Passiflora Edulis f. flavicarpa*). Food Sci Technol 43:1026–1031
51. Vieira AP, Santana SAA, Bezerra CWB, Silva HAS, Chaves JAP, Melo JCP, Silva Filho EC, Airoldi C (2009) Kinetics and thermodynamics of textile dye adsorption from aqueous solution using babassu coconut mesocarp. J Hazard Mat 166:1272–1278
52. Duran CD, Ozdes AG, Sentruk HB (2011) Kinetics and isotherm analysis of basic dyes adsorption on almond shell (*Prunus dulcis*) as a low-cost adsorbent. J Chem Eng Data 56:2136–2147
53. Alkan M, Dogan M, Turhan Y, Demirbas O (2008) Adsorption kinetics and mechanism of maxilon blue 5G dye on sepiolite from aqueous solution. Chem Eng J 139:213–223
54. Tang Y, Zhou Q, Zheng Y, Peng Y (2017) Bio-adsorption of dyes from aqueous solutions by powdered excess sludge (PES): kinectic, isotherm, and thermodynamic study. J Dispersion Sci Technol 38(3):347–354
55. Pathak PD, Mandavgane SA, Kulkarni BD (2016) Characterizing fruit and vegetable peels as biosorbent. Curr Sci 110(11):2114–2123
56. Srivastava VC, Mall ID, Mishra IM (2006) Characterization of mesoporous rice husk ash (RHA) and adsorption kinetics of metal ions from aqueous solution onto RHA. J Hazard Mat B 134:257–267
57. Munagapati VS, Kim DS (2016) Adsorption of anionic azo dye congo red from aqueous solution by cationic modified orange peel powder. J Mol Liq 220:540–548
58. Mokhtari P, Ghaedi M, Dashtian K, Rahimi MR, Purkait MK (2016) Removal of methyl orange by copper sulfide nanoparticles loaded activated carbon: kinetic and isotherm investigation. J Mol Liq 219:299–305
59. Sarma GK, Gupta SS, Bhattacharyya KG (2019) Removal of hazardous basic dyes from aqueous solution by adsorption onto kaolinite and acid-treated kaolinite: kinetics, isotherm and mechanistic study. SN Appl Sci 1:211–225
60. Langmuir I (1918) The adsorption of gases on plane surfaces of glass, mica and platinum. J Am Chem Soc 40(9):1361–1403
61. Nascimento RF, Lima ACA, Vidal CB, Melo DQ, Raulino GSC (2014) Adsorption: theoretical aspects and environmental applications. UFC University Press, Ceará
62. Freundlich HM (1926) Uberdie Adsorption in Losungen. Zeitschrift fur Physikalische Chemie 57(4):385–471
63. Swan E, Urquhart AR (1926) Adsorption equations: a review of the literature. J Phys Chem 31(2):251–276
64. Febrianto J, Kosasih AN, Sunarso J, Ju YH, Indraswati N, Ismadji S (2009) Equilibrium and kinetic studies in adsorption of heavy metals using biosorbent: a summary of recent studies. J Hazard Mat 162:616–645
65. Dabrowski A (2001) Adsorption—from Theory to Practice. Adv Colloid Interface Sci 93:135–224
66. Dubinin MM (1960) The potential theory of adsorption of gases and vapors for adsorbents with energetically non uniform surfaces. Chem Rev 60(2):235–241
67. Hammed BH, Mahmoud DK, Ahmad AL (2008) Sorption equilibrium and kinetics of basic dye from aqueous solution using banana stalk waste. J Hazard Mat 158:499–506
68. Foo KY, Hammed BH (2010) Insights into the modelling of adsorption isotherm systems. Chem Eng J 156:2–10
69. Azari A, Noorisepehr M, Dehghanifardd E, Karimyan K, Hashemi SY, Kalhori EM, Norouzi R, Agarwal S, Gupta VK (2019) Experimental design, modeling and mechanism of cationic dyes biosorption on to magnetic chitosan-lutaraldehyde composite. Int J Biol Macromol 131:633–645
70. Hameed BH, El-Khaiary MI (2008) Malachite green adsorption by rattan sawdust: isotherm, kinetic and mechanism modelling. J Hazard Mat 159:574–579
71. Oliveira CF, Giordani D, Gurak PD, Olivera FC, Marczak LDF (2015) Extraction of pectin from passion fruit peel using moderate electric field and conventional hating extraction methods. Innov Food Sci Emerg Technol 29:201–208
72. Onu EC, Nwabane T (2014) Adsorption studies on the removal of eriochrome black from aqueous solution using Nteje clay. SOP Trans Appl Chem 1(2):14–25
73. Akhaouairi S, Ouachtak H, Ait Addi A, Jada A, Douch J (2019) Natural sawdust as adsorbent for the eriochrome blac T dye removal from aqueous solution. Water Air Soil Pollut 230:181–195
74. Khalid A, Zubair M, Ihsanullal (2018) A comparative study on the adsorption of eriochrome black T dye from aqueous solution on graphene and acid-modified graphene. Arab J Sci Eng 43:2167–2179
75. Zandipak R, Sobhanada-Kani S (2016) Synthesis of NiFe2O4 nanoparticles for removal of anionic dyes from aqueous solution. Desalin Water Treat 57(24):1–13
76. Zubair M, Jarrah N, Manzar MS, Al-Harti M, Daud M, Mu'azu ND, Haladu SA (2017) Adsorption of eriochrome black T from aqueous phase on MgAl-, CoAl-, and NiFe-calcined layered double hydroxides: kinetics, equilibrium and thermodynamic studies. J Mol Liq 230:344–352
77. Ahmaruzzaman M, Ahmed MJK (2015) Begum S (2015) Remediation of eriochrome black T contaminated aqueous solutions using H3PO4-modified berry leaves as a non-conventional adsorbent. Desalination Water Treat 56(6):1–13
78. Wen H, Zhang D, Gu L, Yu H, Pan M, Huang Y (2019) Preparation of sludge-derived activated carbon by fenton activation and the adsorption of eriochrome black T. Materials 12:882–893
79. Blaisi NI, Zubair M, Ihsanullah Ali S, Kazeem TS, Mauzar MS, Al-Kulti W, Al Harthi MA (2018) Date palm ash-MgAl-layered double hydroxide composite: sustainable adsorbent for effective removal of methyl orange and eriochrome black-T from aqueous phase. Environ Sci Pollut Res 25:34319–34331
80. Ho YS (2003) Removal of copper ions from aqueous solutions by tree fern. Water Res 37:2323–2330
81. Ho YS, Chiang CC (2001) Sorption kinetics for dye removal from aqueous solution using activated clay. Sep Sci Technol 36:2473–2488
82. Ho YS, Chiang CC (2001) Sorption studies of acid dye by mixed sorbents. Adsorption 7:139–147
83. Ho YS (2004) Pseudo-isotherms using a second order kinetic expression constant. Adsorption 10:151–158
84. Tan KL, Hameed BH (2017) Insight into the adsorption kinetic models for the removal of contaminants from aqueous solutions. J Taiwan Inst Chem Eng 74:25–48
85. Plazinski W, Rudzinski W, Plazinska A (2009) Theoretical models of sorption kinetics including a surface reaction mechanism: a review. Adv Colloid Interface Sci 152(1–2):2–13
86. Boudouaia N, Bengharez Z, Jellali S (2019) Preparation and characterization of chitosan extracted from shrimp shells waste and chitosan film: application for Eriochrome black T removal

from aqueous solutions. S. Appl Water Sci 9:91. https://doi.org/10.1007/s13201-019-0967-z

87. Ahmad MA, Ahmad N, Os Bello (2015) Adsorption kinetics studies for the removal of synthetic dyes using durian seed activated carbon. J Dispersion Sci Technol 36:670–684
88. Fideles RA, Ferreira GMD, Teodoro FS, Adarme OFH, Silva LHM, Gil LF, Gurgel LVA (2018) Trimellitaded sugarcane bagasse: a versatile adsorbent for removal of cationic dyes from aqueous solution. Part I: Batch adsorption in a monocomponent system. J Colloid Interface Sci 515:172–188
89. Boyd GE, Adamson AW, Myers LS (1947) The exchange adsorption of ions from aqueous solutions by organic zeolites II. Kinetics. J Am Chem Soc 69:2836–2848
90. Reichenberg D (1953) Pointers of ion exchange resins in relation to their structure. Part III. Kinetics of exchange. J Am Chem Soc 75:589–598
91. Hameed BH, El-Khaiary MI (2008) Malachite green adsorption by rattan sawdust: isotherm, kinetic and mechanistic modeling. J Hazard Mat 159:574–579
92. Weber WJ, Weber JC (1963) Kinetics of adsorption on carbon from solution. J Sanit Eng Divi 89(2):31–60
93. Brito SMO, Andrade HMC, Soares LF, Azevedo RP (2010) Brazil nut shells as a new biosorbent to remove methylene blue and indigo carmine from aqueous solution. J Hazard Mat 174:84–92